EARTH SURFACE PROCESSES AND LANDFORMS
Earth Surf. Process. Landforms **38**, 1714–1724 (2013)

Published online 16 April 2013 in Wiley Online Library
(wileyonlinelibrary.com) DOI: 10.1002/esp.3421

Shear velocity estimates in rough-bed open-channel flow

Fereshteh Bagherimiyab* and Ulrich Lemmin
ENAC, Ecole Polytechnique Fédérale de Lausanne (EPFL), Lausanne, Switzerland

Received 10 May 2012; Revised 5 March 2013; Accepted 6 March 2013

*Correspondence to: F. Bagherimiyab, ENAC, Ecole Polytechnique Fédérale de Lausanne (EPFL), Station 18, CH-1015 Lausanne, Switzerland. E-mail: fereshteh.bagherimiyab@gmail.com

ESPL
Earth Surface Processes and Landforms

ABSTRACT: Shear velocity u_* is an important parameter in geophysical flows, in particular with respect to sediment transport dynamics. In this study, we investigate the feasibility of applying five standard methods [the logarithmic mean velocity profile, the Reynolds stress profile, the turbulent kinetic energy (TKE) profile, the wall similarity and spectral methods] that were initially developed to estimate shear velocity in smooth bed flow to turbulent flow over a loose bed of coarse gravel ($D_{50} = 1{\cdot}5$ cm) under sub-threshold conditions. The analysis is based on quasi-instantaneous three-dimensional (3D) full depth velocity profiles with high spatial and temporal resolution that were measured with an Acoustic Doppler Velocity Profiler (ADVP) in an open channel. The results of the analysis confirm the importance of detailed velocity profile measurements for the determination of shear velocity in rough-bed flows. Results from all methods fall into a range of $\pm$ 20% variability and no systematic trend between methods was observed. Local and temporal variation in the loose bed roughness may contribute to the variability of the logarithmic profile method results. Estimates obtained from the TKE and Reynolds stress methods reasonably agree. Most results from the wall similarity method are within 10% of those obtained by the TKE and Reynolds stress methods. The spectral method was difficult to use since the spectral energy of the vertical velocity component strongly increased with distance from the bed in the inner layer. This made the choice of the reference level problematic. Mean shear stress for all experiments follows a quadratic relationship with the mean velocity in the flow. The wall similarity method appears to be a promising tool for estimating shear velocity under rough-bed flow conditions and in field studies where other methods may be difficult to apply. This method allows for the determination of u_* from a single point measurement at one level in the intermediate range ($0{\cdot}3 < h < 0{\cdot}6$). Copyright © 2013 John Wiley & Sons, Ltd.

KEYWORDS: rough-bed open-channel flow; Reynolds stress; TKE; shear velocity; bed shear stress; turbulence spectra; ADVP

Introduction

Bed shear stress τ is an important parameter in many geophysical and environmental engineering applications. It is a fundamental variable and turbulence scaling parameter in river studies because it relates to scour and channel changes. The estimation of critical erosion and deposition thresholds and of erosion and deposition rates requires the determination of hydrodynamic forces applied to sediment as bed shear stress. The accuracy of sediment transport rate calculations is strongly affected by shear stress estimates. Bed shear stress τ is related to shear velocity u_* by $\tau = \rho\, u_*^2$, where ρ is water density. Shear velocity is linked to turbulent flow structures close to the bed and is important for understanding the development of near-bed turbulence. In gravel-bed flows, shear stress cannot be measured directly and is indirectly determined from estimates of u_*. Due to the quadratic relationship between τ and u_*, high-quality estimates of u_* are required in order to obtain reliable shear stress estimates.

Shear velocity is determined using velocity profile data, particularly those measured in the inner layer. In loose gravel bed flows, a roughness layer develops just above the bed (Raupach, 1981; Nikora and Smart, 1997), thus affecting the lower end of the inner layer velocity profile. The flow dynamics in the roughness layer are directly influenced by the length scales associated with bed roughness elements and this flow is often three–dimensional (3D). No universal concept exists for the determination of the layer height. A wide range of propositions for the layer height is found in the literature: 50 roughness lengths z_0, Townsend (1976); two to five diameters D, Raupach *et al.* (1991); three diameters D, Wilcock (1996); σ_D (σ_D = standard deviation of the bed elevations), Nikora and Goring (2000); $0{\cdot}05\, h$ (h is water depth), Smart (1999). Above the roughness layer, concepts of smooth boundary layer flow may be applied to characterize the flow. Their applicability also depends on the relative roughness D/h. If the relative roughness increases, the height of the water column may not be sufficient for the boundary layer profiles to develop according to known smooth bed flow distribution laws. Katul *et al.* (2002) suggest that these laws may fail for $h < 10D$.

Shear velocity in rough-bed flows often has to be determined from detailed full depth velocity profiles because of the uncertainty of the roughness layer height. In gravel bed rivers, Wilcock (1996) and Smart (1999) used the logarithmic profile method to determine shear velocity, Nikora and Goring (2000) applied the Reynolds stress method and MacVicar and

Roy (2007) applied the turbulent kinetic energy (TKE) method. Rowinski *et al*. (2005) compared these methods in a laboratory study of flow over armoured gravel beds and found that the logarithmic profile method was not suitable in their case. They pointed out that due to the bed irregularity in coarse gravel beds, it is difficult to use single point measurements for the determination of shear velocity with the methods which they applied.

Under certain conditions, it may be difficult to obtain reliable velocity profile data, particularly in the field. In that case, shear velocity must be estimated from single point measurements. This approach is often taken in oceanographic studies (Stapleton and Huntley, 1995). Kim *et al*. (2000) used the same methods as Rowinski *et al*. (2005) and the spectral method in an estuary over a soft mud bottom and recommend further investigating the TKE method based on velocity measurements carried out at two levels. Biron *et al*. (2004) performed laboratory experiments over fine sand, using the same methods and observed that the logarithmic profile methods gave shear velocity estimates that were significantly larger than the remaining methods. They suggest that single point measurements should be made at 0·1 h, but above the roughness layer. However, they caution that more research is needed to determine whether this level is correct for all flow cases. Hurther and Lemmin (2000) investigated the validity of the wall similarity method over transitionally rough beds based on detailed profile data. They found this method promising for applications in difficult bed conditions, because it allows determining the shear velocity from single point measurements within the intermediate depth range. It appears that no study thus far has compared all these methods in flows over fully rough beds with coarse gravel, even though this situation is most often found in rivers with irregular bed surfaces.

Since the laboratory studies cited earlier were carried out under less rough-bed flow conditions ($D_{50} < 0{\cdot}5$ cm) and found great differences in the shear velocity estimates calculated by different methods, it is of interest to investigate the feasibility of using these methods under coarse gravel bed conditions. In this study, local mean shear velocity estimates are calculated using Acoustic Doppler Velocity Profiler (ADVP) quasi-instantaneous full depth profile data that were collected under controlled laboratory conditions in a sub-threshold open-channel flow over a fully rough coarse gravel-bed ($D_{50} = 1{\cdot}5$ cm). We will first summarize the methods used. We will then investigate the possibility of applying them to turbulent flow over a fully rough bed. The results obtained by the different methods will be compared and discussed. The objective is to determine the best of these methods and make recommendations on each of them. Furthermore, profile methods will be applied here in order to determine which of these methods can also provide reliable shear velocity estimates based on single point measurements.

Techniques for estimating shear velocity

Shear velocity was initially defined within concepts of boundary layer flow. Commonly employed methods are based on the assumption of the presence of a constant shear layer stress within the water column where shear stress only varies slightly from bottom stress τ. Even though a constant shear layer does not exist in open-channel flow, these methods have been successfully applied in open-channel flow studies. For open-channel flow over rough beds, Nezu and Nakagawa (1993) suggest four methods to calculate shear velocity and bed shear stress: (1) from the bed slope under conditions of normal and uniform flow, (2) the logarithmic profile method, (3) the Reynolds stress method, and (4) direct measurements.

In two-dimensional (2D), uniform flow, shear velocity can be estimated based on a force balance approach and is often used as a reference:

$$u_* = \sqrt{g\,R\,I} \tag{1}$$

where g is the gravitational acceleration, R the hydraulic radius and I the bed slope. However, this method provides an overall value and may not be adequate for the evaluation of the flow characteristics. In fully rough flows, local estimates of shear velocity that determine sediment dynamics may strongly deviate from those obtained from Equation 1 due to significant bed roughness variability. In the present study, we focus on profile methods for the determination of u_*, taking advantage of the detailed quasi-instantaneous full-depth ADVP profiles of all three velocity components. We will evaluate methods (2) and (3) and in addition, apply the TKE method, the wall similarity method and the spectral method.

Logarithmic velocity profile method

Katul *et al*. (2002) suggest that a logarithmic velocity profile may exist in the inner layer of rough-bed flows covering the lowest 20% of the water depth, if $h > 10D$. The logarithmic velocity distribution is described by the von Karman–Prandtl equation (Schlichting, 1987):

$$\frac{u}{u_*} = \frac{1}{\kappa}\ln\left(\frac{z}{z_0}\right) \tag{2}$$

The constant κ is von Karman's constant. We will use $\kappa = 0{\cdot}4$ (Smart, 1999). Flow dependence of κ is discussed in Ferreira *et al*. (2012). Here, z_0 is the characteristic hydraulic roughness length (or roughness), and u is the mean longitudinal velocity at height z above the bed. Monin and Yaglom (1971) define z_0 as the height at which the mean velocity of the flow will become zero, if the logarithmic law would be applicable down to that height. In rough-bed flows, the relative magnitude of z_0 and a representative length scale for the roughness elements are important for the determination of the lower limit of the validity of the log-law. For homogeneous sand roughness, Monin and Yaglom (1971) established $z_0/D_{50} = 1/30$ with bed roughness parameter D_{50}. For irregular roughness, the proportionality coefficient is often larger: $z_0/D_{50} \approx 1/10$ or even $z_0/D_{50} \approx 1/5$ (Monin and Yaglom, 1971; Townsend, 1976). These authors stress that this coefficient may not strictly be a constant for a set of irregularities, since it also depends on the form of the roughness element.

The logarithmic velocity profile method is widely used in open-channel flow and river studies (Nezu and Nakagawa, 1993). It has the advantage that no independent estimate of z_0 is needed, because u_* only depends on the slope of the profile, not the intercept. In rough-bed flows, a logarithmic profile will develop above the roughness layer. The following ranges have been proposed for the validity of the log law: at heights of $z/z_0 > 50$ (Townsend, 1976), between 3 $D_p < z < h/5$ (D_p being the grain size for which p percent is finer; often taken as D_{84}; Wilcock, 1996), 0.05 $h < z < h/2$ (Smart, 1999).

Reynolds stress method

When turbulence measurements are available, local mean shear velocity can be determined from the measured Reynolds stress distribution in the constant stress layer where stress within the water column only varies slightly from bottom stress τ (Kim *et al.*, 2000). It can be expressed as:

$$u_* = \sqrt{-\ \overline{u'w'}} \tag{3}$$

where u' and w' are the velocity fluctuations of the longitudinal (streamwise) and vertical components, respectively. The overbar denotes time mean values. Due to internal shear within the measuring volume, acoustic Doppler instrument measurements are less reliable in strong velocity gradient layers, such as the one close to the bed (Lhermitte and Lemmin, 1994, Dombroski and Crimaldi, 2007). This method is also sensitive to deviations from 2D uniform flow (Nezu and Nakagawa, 1993; Kim *et al.*, 2000; Nikora and Goring, 2000; Albayrak and Lemmin, 2011) and a precise sensor alignment is required. In rough-bed open-channel flow, Reynolds stress varies linearly in the outer layer (Nezu and Nakagawa, 1993). These authors and Nikora and Goring (2000) suggested using the extrapolation of the Reynolds stress profile to the bed,

$$u_* = \sqrt{\left(-\ \overline{u'w'}\right)_{z\to 0}} \tag{4}$$

In addition, this method allows verifying the 2D flow conditions by a linear distribution of the Reynolds stress above the maximum.

Turbulent kinetic energy (TKE) method

Bed shear stress can be obtained from turbulent velocity fluctuations through TKE calculations. TKE is defined as:

$$TKE = {}^1\!/_2\ \left(\overline{u'^2} + \overline{v'^2} + \overline{w'^2}\right) \tag{5}$$

where v' is the fluctuating transversal velocity component. Linear relationships between TKE and shear stress have been formulated (Townsend, 1976). Soulsby (1980) found that the average ratio of shear stress to TKE is constant

$$|\tau| = C_1\ \rho\ TKE \tag{6}$$

Therefore,

$$|u_*| = \sqrt{C_1\ \ TKE} \tag{7}$$

where C_1 is a proportionality constant. For oceanic conditions, Soulsby (1980) suggested $C_1 \approx 0.2$ while Stapleton and Huntley (1995) applied $C_1 \approx 0.19$ which is also used for atmospheric boundary layers. The value $C_1 \approx 0.19$ was used by MacVicar and Roy (2007) in a gravel bed river, by Rowinski *et al.* (2005) in a rough-bed open-channel, and by Pope *et al.* (2006) in river and laboratory studies. Wolf (1999) proposed C_1 0·19 based on coastal ocean studies. Kim *et al.* (2000) found $C_1 \approx 0.21$ in an estuary by best fit to the data, suggesting that further studies are needed to confirm that this is can be considered as a universal constant in hydraulics.

Kim *et al.* (2000) assumed a linear relationship between the TKE and the variances (hereinafter labeled TKE W′), and suggested that shear stress may be related to the vertical variance component

$$|\tau| = C_2\ \rho\ \overline{w'^2} \tag{8}$$

$$|u_*| = \sqrt{C_2\ \overline{w'^2}} \tag{9}$$

Kim *et al.* (2000) proposed $C_2 \approx 0.9$ by comparing the results of TKE W′ with the results from the other methods.

Nezu and Nakagawa (1993) have shown that Reynolds stress and TKE are correlated in open-channel flow. In the inner layer, the correlation coefficient $R = \left(-\overline{uw}\ /2\ TKE\right)$ has a value close to 0·1. This results in $-\overline{uw}\ \approx 0.2\ TKE$. As with the Reynolds stress method, by an extrapolation of the TKE profile to the bed, we obtain

$$u_* \approx \sqrt{0.2\ TKE}_{\ z\to 0}. \tag{10}$$

Wall similarity method

The wall similarity concept in turbulent boundary layer flow under uniform flow conditions at high Reynolds numbers implies that an extended depth range exists where turbulent energy production and dissipation are nearly in equilibrium and diffusion is negligible, independent of flow and bed roughness conditions. In the equilibrium layer ($0{\cdot}15 \le z/h \le 0{\cdot}6$), a balance exists between production p and energy dissipation ε that is given by (Townsend, 1976)

$$-p + \varepsilon = \overline{u'\ w'}\ \ (\partial u/\partial z) + \varepsilon = 0 \tag{11}$$

and the turbulent energy diffusion term is

$$\frac{\partial}{\partial z}\left[\frac{1}{2}\ \overline{\left(u'^2 + v'^2 + w'^2\right)w'}\ \right] \approx 0 \tag{12}$$

Thus, the vertical flux of TKE $\frac{1}{2}\ \overline{\left(u'^2 + v'^2 + w'^2\right)w'} \cong const$ in the equilibrium layer. Hurther and Lemmin (2000) have shown that the vertical flux of TKE normalized by the cube of the shear velocity is given by

$$\frac{1}{2\ u_*^3}\ \overline{\left(u'^2 + v'^2 + w'^2\right)\ w'} = F_k \tag{13}$$

This normalization takes into account the bed roughness effect. The following equation for u_* is then obtained:

$$u_* = \left(\frac{1}{2\ F_k}\ \overline{\left(u'^2 + v'^2 + w'^2\right)w'}\right)^{1/3} \tag{14}$$

F_k was found to be a constant with a mean value of 0·3 for the range $0{\cdot}15 \le z/h \le 0{\cdot}6$ (Lopez and Garcia, 1999; Hurther and Lemmin, 2000). Therefore, an estimate of the bottom friction velocity can be obtained from a single determination of the vertical turbulent energy flux at any level within the range $0{\cdot}15 \le z/h \le 0{\cdot}6$. Since this range is fairly wide, a precise knowledge of the measurement depth or the bed reference level is not necessary for determining u_* by this method. Due to the one-third power relationship, the wall similarity method is not overly sensitive to errors in the determination of the energy flux. It is therefore well suited for field measurements. The wall similarity method can be further simplified by only measuring a time series of u', if the empirical relations between the turbulence intensities exist ($\sqrt{\overline{v'^2}/\overline{u'^2}} = 0.75$ *and* $\sqrt{\overline{w'^2}/\overline{u'^2}} = 0.35$; Raupach, 1981, Hurther *et al.*, 2007). We will investigate the validity of these relationships in our analysis.

Spectral method

Shear velocity can be obtained from the spectra of the turbulent velocity fluctuations. In the log-law layer, where the spectral range of production, p, is well separated from that of energy dissipation ε, an inertial subrange is established between the two. If there are no sources or sinks of energy in the inertial subrange, then the spectrum of a velocity component in the inertial subrange has the following form (Hinze, 1975, Stapleton and Huntley, 1995, Kim *et al.*, 2000):

$$\phi_{ii}(k) = a_i\,\varepsilon^{2/3}\,k^{-5/3} \tag{15}$$

where $\phi_{ii}(k)$ is the spectral density of the ith velocity component at wavenumber k, and a_i is the one-dimensional (1D) Kolmogorov constant. For locally isotropic turbulence, $a_1 \approx 0.51$ (Kaimal *et al.*, 1972) and $a_2 \approx a_3 = 4/3\ \ a_1 \approx 0.69$ (Tennekes and Lumley, 1972). These values were used in the ocean (Stapleton and Huntley, 1995) and by Kim *et al.* (2000) in the estuary. Grant *et al.* (1984) suggested $a_3 \approx 0.50$ in their continental shelf study. For velocity data obtained in the time domain, frequency spectra have to be transferred into wavenumber spectra with $k = 2\pi\ f/u$; f is the frequency and u the convection velocity. Under the condition of $k\ \phi_{ii}(k)/u^2 << 1$, Taylor's 'frozen turbulence' hypothesis can be applied (Kim *et al.*, 2000).

For a logarithmic profile region with a constant stress layer, one can obtain u_* from Equation 11 together with Equation 3 and $\partial u/\partial z = u_*/\kappa z$ (Kim *et al.*, 2000) as

$$u_* = (\varepsilon\,\kappa\,z)^{1/3} \tag{16}$$

By combining Equations 15 and 16, u_* for the vertical velocity component is given by

$$u_* = (\kappa\,z)^{1/3}\left(\frac{\phi_{33}(k)\,k^{5/3}}{a_3}\right)^{1/2}. \tag{17}$$

This method of estimating shear velocity u_* has mainly been used in oceanography. It can provide estimates based on measurements at a single depth and it is less sensitive to errors in sensor alignment than the Reynolds stress method. We will investigate the suitability of this method in open-channel flow.

Experiments

Experimental set-up

Experiments were carried out in a 2·4 m wide by 27 m long open-channel with a 10 cm thick bed of loose mixed gravel with $D_{50} = 1{\cdot}5$ cm (Figure 1a), representing gravel beds found in rivers. There is no sand in the mixture. Initially, the permeable gravel bed was created and leveled by hand along the channel. It did not move during the experiments. This was manually controlled during the series of experiments at several locations along the channel. However, small local level changes were observed between experiments. Measurements were made 12 m from the channel entrance where the turbulent flow is fully developed for two flow depths ($h = 19$ and 20 cm, respectively) and with Reynolds numbers ranging from $3{\cdot}24 \times 10^4$ to $1{\cdot}07 \times 10^5$. The flow depth was maintained by a manually operated tailgate. The channel has a zero slope angle.

Acoustic Doppler Velocity Profiler (ADVP)

The ADVP measures quasi-instantaneous profiles of all three velocity components over most of the water depth of an open-channel flow along a single straight vertical line of consecutive scattering volumes (Shen and Lemmin, 1997). Thus, all points in the profiles were nearly simultaneously measured during a single recording. Four wide-angle receiver transducers are placed symmetrically around a central emitter (Figure 1b). The transducers are arranged in two perpendicular planes, each of which allows resolving profiles of one horizontal component and the vertical velocity component. Thus, two simultaneous profiles of the vertical component are taken in the same measuring volumes. The redundancy of the vertical component profiles allows controlling the quality of the geometrical alignment of the transducers, both in the horizontal and the vertical plane (Hurther and Lemmin, 2001). This is important for the application of the Reynolds stress and the TKE methods.

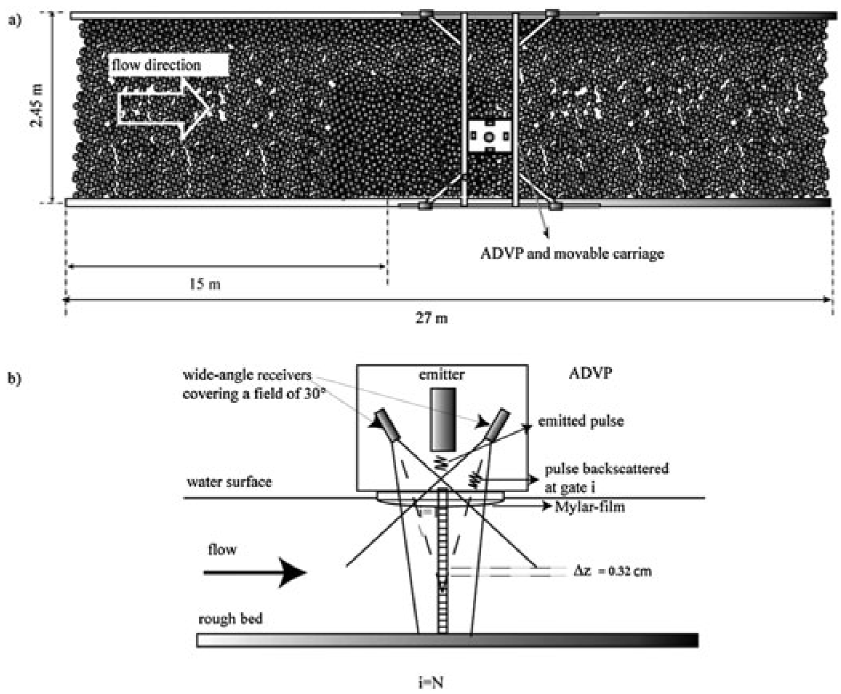

Figure 1. Schematics of (a) the hydraulic open channel, and (b) the ADVP instrument.

Complete three-dimensional (3D) Doppler phase profiles are sampled at 1000 Hz. Velocity profiles are obtained from these data by the pulse-pair method (Lhermitte and Lemmin, 1994) averaged over 32 pairs. The resulting spatio-temporal resolution (3·2 mm and 0·032 seconds, respectively) is sufficient to quantitatively estimate turbulence parameters in the productive and inertial ranges of the spectral space.

Procedure

In this study, a series of nine experiments at different Reynolds numbers for two slightly different flow depths was conducted (Table I). Due to the zero bed slope, the flow is in a state that Yaglom (1979) has termed as 'moving equilibrium.' In this state, the variation of water depth and shear velocity in the downstream direction is sufficiently slow and can be ignored. A zero-pressure gradient condition (or uniform flow condition) was verified in the working section by taking profiles over a range of 2·5 m along the channel axis. In this case, u_* can be considered as a local value for a given location. Both flow depths have approximately the same relative roughness (D_{50}/h 0·075). We observed that relative roughness had no effect on the validity of the results presented here down to $D_{50}/h \approx 0{\cdot}125$. For $D_{50}/h \approx 0{\cdot}075$, ADVP measurements resulted in profiles with approximately 50 sampling volumes in the water column, thus allowing for a detailed profile analysis. Data were collected for three minutes in the center of the channel.

Measured profiles were cut at $z/h = 0{\cdot}9$, since a thin boundary layer in the near surface water layer is generated by the instrument housing (Figure 1b; Hurther *et al.*, 2007). The bottom level was identified from the velocity information ($u = 0$), and confirmed by the corresponding change of backscatter intensity. The sampling volume height is $\Delta z = 3.2$ *mm*. The origin of the coordinate system was placed at 1/2 Δz of the lowest sampling volume (1/2 $\Delta z \approx 0.1$ D_{50}). Water depth was measured as the distance between this level and the housing at the surface. The collected data were first de-aliased (Franca and Lemmin, 2006) to remove spikes and subsequently de-noised using the redundant information of the vertical velocity in the two planes (Hurther and Lemmin, 2001). Measured velocities have an error of the order $O(2 \div 3\ mms^{-1})$ (Blanckaert and Lemmin, 2006, Hurther *et al.*, 2007). For the present analysis, the vertical velocity that was measured in the longitudinal plane was used. The measured velocities were decomposed into a mean (u for streamwise, w for vertical) and a fluctuating component (u' for streamwise, w' for vertical) by Reynolds decomposition.

Results

Logarithmic profile method

Representative profiles for the lower 0·4 z/h are given in semi-logarithmic form (Figure 2). The linear least-square fit of Equation 2 to these data is shown as a solid line and it can be seen that the fit closely follows the measured mean longitudinal velocity profiles. Very close to the bed, typically for the lowest two or three points in the profile, a deviation from the logarithmic law is observed due to the presence of the roughness layer. In the roughness layer, individual roughness elements may affect the flow structure and the flow may become 3D (Nikora and Goring, 2000). The thickness of the roughness layer defined by three profile points is $\approx 0{\cdot}05\,h$, as was suggested by Smart (1999). This layer thickness corresponds to about

Table I. Experimental conditions and estimates of shear velocity u_* determined by different methods

						Methods for u_* (cm s^{-1}) calculations							
Experiment	Water depth, h (cm)	$\bar{U}$ (cm s^{-1})	Reynolds number	F_r	z_0 (cm)	Logarithmic	Reynolds	Wall similarity	TKE, $C_1 = 0{\cdot}19$	TKE W′, $C_2 = 0{\cdot}9$	Spectral	Mean	Standard deviation
1	19	36·63	$6{\cdot}93 \times 10^4$	0·27	0·029	2·92	2·64	2·16	2·37	2·45	2·65	2·53	0·21
2	20	45·79	$9{\cdot}12 \times 10^4$	0·33	0·002	2·26	2·94	3	3·16	2·48	3·20	2·84	0·38
3	20	50·2	$1{\cdot}00 \times 10^5$	0·36	0·0025	2·72	3·32	3·4	3·32	2·98	3·30	3·17	0·27
4	20	53·21	$1{\cdot}06 \times 10^5$	0·38	0·005	3·57	3·66	3·6	3·62	2·99	3·36	3·61	0·26
5	19	17·12	$3{\cdot}24 \times 10^4$	0·12	0·061	1·18	1·58	1·15	2·30	1·18	2·44	1·64	0·59
6	19	34·82	$6{\cdot}59 \times 10^4$	0·26	0·025	2·65	3·04	2·3	2·57	2·67	2·70	2·66	0·24
7	19	41·38	$7{\cdot}83 \times 10^4$	0·30	0·04	3·23	2·71	2·6	2·77	2·32	3·45	2·85	0·42
8	19	49·09	$9{\cdot}29 \times 10^4$	0·36	0·06	3·98	3·24	3·3	3·24	2·73	3·54	3·34	0·41
9	19	56·54	$1{\cdot}07 \times 10^5$	0·41	0·03	4·37	3·79	3·5	3·79	3·37	4·41	3·87	0·43

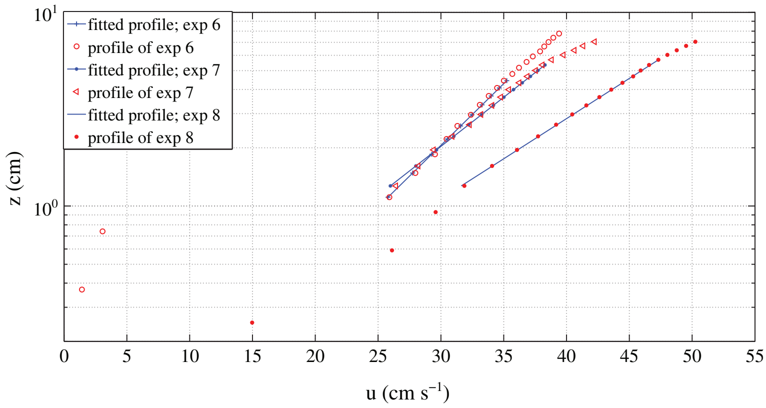

Figure 2. Logarithmic profile method for different experiments with water depth $h = 19$ cm. The range over which the data are fitted is indicated for each experiment. This figure is available in colour online at wileyonlinelibrary.com/journal/espl

$0{\cdot}7D_{50}$ which is smaller than the $2D_{50}$ to $5D_{50}$ proposed by Raupach *et al.* (1991) or the $3D_{50}$ proposed by Wilcock (1996).

The vertical extent of the height of the logarithmic layer was determined by stepwise extending the linear least square fitting range. For each profile, a fitting loop was started from the first point above the roughness layer and consecutively included the next higher data point in the profile into the fitting procedure. In each step, the shear velocity u_* and the regression coefficient of the fitting were determined. With each new data point added, u_* increases. Over the range 0·05–0·4 z/h, the increase in u_* is of the order O(10%). The regression coefficient R^2 is always relatively high (> 0·9). However, the regression coefficient R^2 goes through a maximum between $z/h = 0{\cdot}25$ and $z/h = 0{\cdot}3$. Around the maximum of R^2, u_* values remain nearly constant and slightly increase again above $z/h = 0{\cdot}35$. Even though a logarithmic fit still appears to be reasonable beyond 0.3 z/h, the regression coefficient analysis indicates that the height of the logarithmic layer should be limited to $z/h \approx 0{\cdot}25$. This value is larger than the limit of $z/h = 0{\cdot}2$ given for the validity of the logarithmic law (Monin and Yaglom, 1971; Nezu and Nakagawa, 1993). However, it is smaller than $z/h = 0{\cdot}5$, as suggested by Smart (1999). For the determination of u_* and z_0, the layer height corresponding to the maximum of R^2 was taken.

Smart (1999) indicated that a wide range of z_0 can be expected in rough-bed flows. In these flows, the roughness length will be affected by the dimension of the bed material at the base of the profile and the form of the roughness element composition. It will also be affected by the bed conditions upstream of the velocity profile location. The ratio between the physical roughness height z_0 and D_{50} falls into the range given by Smart (1999), but it is smaller than $z_0/D_{50} \approx 1/10$, as was suggested for flows over irregular rough surfaces (Monin and Yaglom, 1971; Townsend, 1976).

No relative errors in z occur, since the ADVP takes full depth velocity profiles in one recording. Thus, the profile fitting in this study is more robust than in the case of individual point-by-point measurements. Furthermore, the range of the profile that is fitted to Equation 2 is composed of at least 10 points in all experiments. This significantly reduces the error of the estimates (Wilkinson, 1983).

Reynolds stress method

The Reynolds stress was calculated for all points in the profile up to $0{\cdot}9z/h$. Typical Reynolds stress profiles (Figure 3) reasonably follow a linear distribution above the maximum, indicating that the flow is 2D. In order to determine u_*, the profile above the maximum was approximated by a linear fit that is extrapolated to level $z = 0$ (Nezu and Nakagawa, 1993; Nikora and Goring, 2000). A maximum in the Reynolds stress distribution is observed at around $0{\cdot}2z/h$ in all experiments, except experiment 6 (Figure 3), where it is slightly shifted upwards. This shift may be due to longitudinal secondary current cells previously observed in this channel that may cause a deviation from the 2D profile and also affect the shear velocity under certain flow conditions (Nezu and Nakagawa, 1993; Albayrak and Lemmin, 2011).

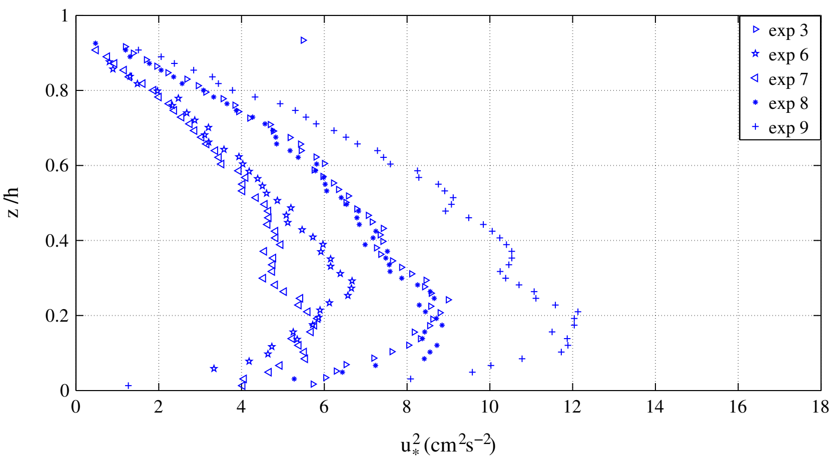

Figure 3. Reynolds stress profiles obtained from ADVP data with water depth $h = 19$ cm for different experiments. This figure is available in colour online at wileyonlinelibrary.com/journal/espl

TKE method

The TKE and the variance of the vertical component (hereinafter labeled TKE W′) were calculated for all data points and the profiles were again limited to 0·9*z/h*. TKE profiles peak at around 0·1*z/h* (Figure 4), as has previously been observed for less rough-bed conditions (Nicholas, 2001; Biron *et al.*, 2004). Above the maximum, TKE profiles closely follow the Reynolds stress profiles in their linear form. For all experiments, the form of the TKE W′ profile is different from that of the TKE method (Figure 4). The short range above the maximum is not well suited for linear fitting. Therefore, the estimates based on the TKE W′ fitting have to be considered less reliable than full TKE estimates. Kim *et al.* (2000) who suggested the TKE W′ method, applied it to single point measurements and not to profiles.

Wall similarity method

Results using the wall similarity method with $F_k = 0{\cdot}3$ are presented in Figure 5. It can be seen that over the range $0{\cdot}25 \le z/h \le 0{\cdot}7$, u_* values remain almost constant. This indicates a nearly constant vertical flux of TKE over this layer, thus confirming the validity of the wall similarity method in our fully rough flow. In the layer below, in particular below $z/h \le 0{\cdot}1$, the values are erratic, indicating the effect of the roughness layer. Therefore, measurements at any level between $0{\cdot}25 \le z/h \le 0{\cdot}7$ can be used for the determination of u_*. It was found that $\sqrt{\overline{v'^2}/\overline{u'^2}} < 0.75$ and $\sqrt{\overline{w'^2}/\overline{u'^2}} < 0.35$ in all flow cases studied here. As a consequence, using the relation, $\sqrt{\overline{v'^2}/\overline{u'^2}} = 0.75$ and $\sqrt{\overline{w'^2}/\overline{u'^2}} = 0.35$ (Raupach, 1981, Hurther *et al.*, 2007), will result in estimates for u_* that are too high.

Spectral method

Energy density spectra were calculated for all sampling volumes of the profiles. In all spectra, except for those close to the bed ($z/h \le 0{\cdot}054$), an inertial range was well developed. Shear velocity was calculated for the spectra of the longitudinal and the vertical velocity components (Figure 6). It was found that this method often gives poor results for the longitudinal component, thus making it difficult to determine reliable values for $\phi_{11}(k)\,k^{5/3}$. Therefore, these results were omitted from the analysis. In order to determine the reference depth for a representative u_*, shear velocity estimates were calculated from the spectra of the vertical velocity component for all measurement levels in each profile. Results for the lower 0·4*z/h* in Figure 7 show that u_* continuously increases with height above the bed throughout the logarithmic layer. This corresponds to a rise in the spectral energy level with height above the bed. The overall pattern is similar for all experiments. Kim *et al.* (2000) made estimates for the heights of 14 and 44 cm above the

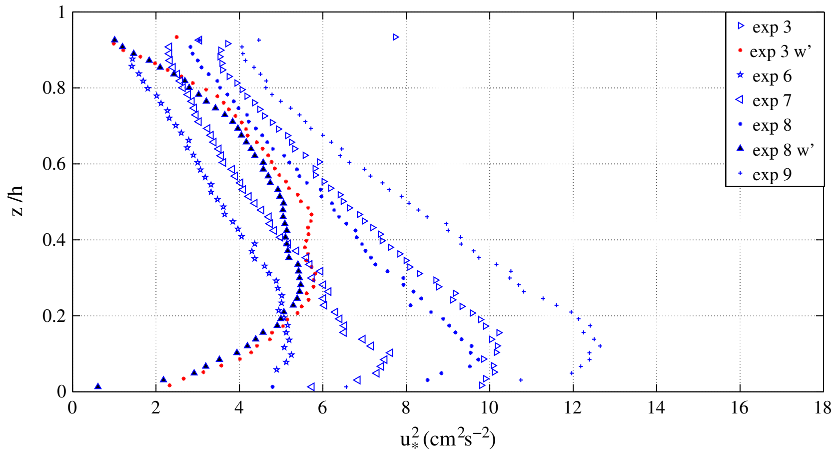

Figure 4. TKE and TKE W′ profiles obtained from ADVP data with water depth $h = 19$ cm for different experiments. This figure is available in colour online at wileyonlinelibrary.com/journal/espl

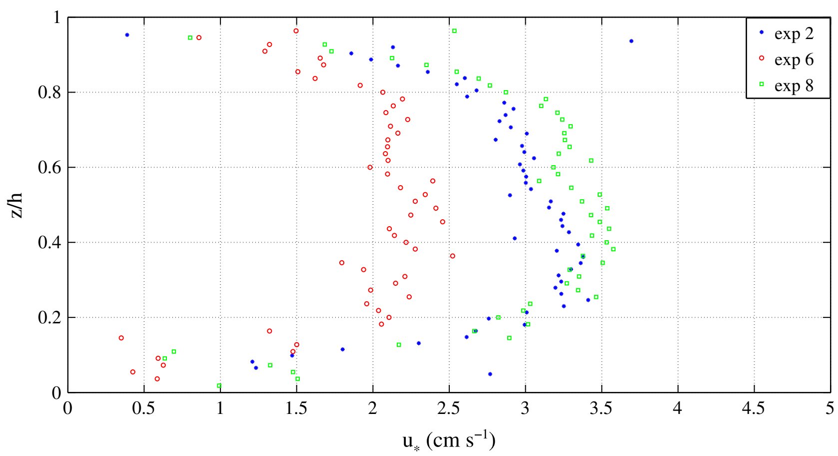

Figure 5. Shear velocity estimates obtained by the wall similarity method for different experiments. This figure is available in colour online at wileyonlinelibrary.com/journal/espl

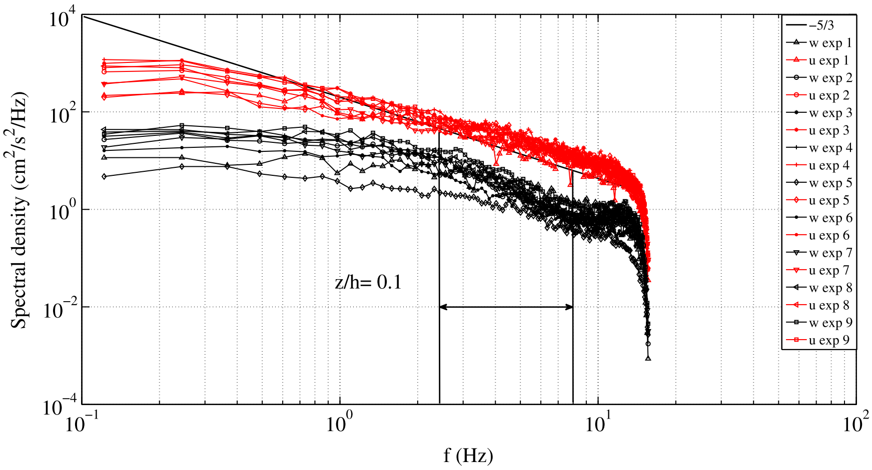

Figure 6. Typical energy spectra for the streamwise and the vertical velocity components at $z/h = 0{\cdot}1$ for different experiments. The inertial subrange is indicated by vertical lines. This figure is available in colour online at wileyonlinelibrary.com/journal/espl

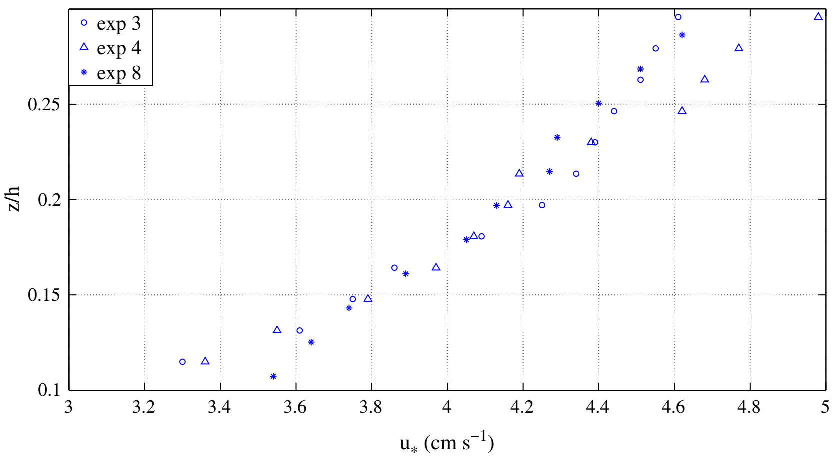

Figure 7. Shear velocity u_* obtained from spectra of the vertical velocity component for different experiments in the range $0{\cdot}1 < z/h < 0{\cdot}3$. This figure is available in colour online at wileyonlinelibrary.com/journal/espl

bed, and observed a 22% increase in u_* for the higher of the two points.

In order to determine the height of representative u_* values, one may compare u_* values obtained from the spectral method at different heights above the bed within the log layer to those obtained by the methods discussed earlier (Table I). For experiment 1, a u_* value at $0{\cdot}2z/h$ is closest to the values given in Table I. In the remaining experiments, best agreement is found for u_* values close to $0{\cdot}1z/h$. These values are included in Table I.

Discussion

In this study, we analyzed various profile methods to determine shear velocity, taking advantage of the quasi-instantaneous profiling capacity of the ADVP. For each flow case, all methods were evaluated based on the same detailed profile data. The shear velocity values obtained using the different methods for all the experiments are summarized in Table I. The results cover a wide range of Reynolds numbers and thus flow velocities. As can be expected for such rough-bed flow, shear velocity estimates obtained by different methods for a given flow case rarely coincide and no systematic trend between the results of the different methods is obvious. However, some tendencies are observed in the results. Nezu and Nakagawa (1993) suggested that the extrapolated Reynolds stress method gives the most reliable estimates. Biron *et al.* (2004) and Rowinski *et al.* (2005) used the Reynolds stress method as a reference to compare with results obtained by other methods. When results from other methods are plotted against those from the Reynolds stress method (Figure 8), no clear trend or tendency can be seen over the range investigated here. Results fall randomly on both sides of the 1:1 line.

The logarithmic profile method is often used, because it is based on the mean velocity profile and has good accuracy in simple flow cases (Wilcock, 1996). In four of the nine experiments, logarithmic profile method estimates are higher, but in the remaining cases they are lower than the Reynolds stress method estimates (Figure 8). Rowinski *et al.* (2005) observed systematically higher values for the logarithmic method and they concluded that this method was not suitable for their rough-bed flow conditions. Biron *et al.* (2004) found the highest estimates for the logarithmic law method in the sand bottom study. In our case, the relative roughness is $D_{50}/h \approx 0{\cdot}75$ and thus $h \approx 13{\cdot}3D_{50}$, which should allow the use of the logarithmic profile method (Katul *et al.*, 2002). The high regression coefficients found in the fitting procedure to the logarithmic profile suggest that the data are of good quality and that a logarithmic profile is well developed in the inner layer. Smart (1999) pointed out that variation in the upstream bed conditions might also influence the results.

The differences between the results of the TKE method and the Reynolds stress method are generally less than 10% (Figure 8). In five experiments, the two methods give similar

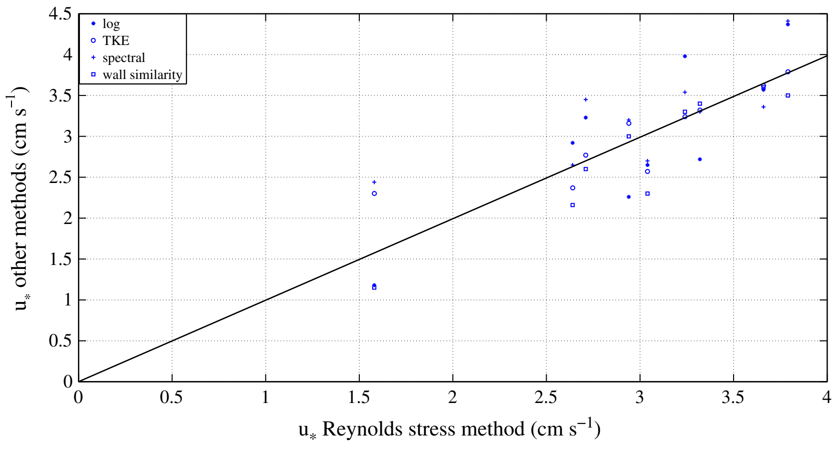

Figure 8. Comparison of shear velocities estimated from all methods. This figure is available in colour online at wileyonlinelibrary.com/journal/espl

results. For the slowest flow case (experiment 5), a noisy TKE profile produced the greatest difference (about 40%). The coefficient $C_1 \approx 0{\cdot}19$ in the TKE method was taken from the literature and applied to this rough-bed flow. Rowinski *et al.* (2005) used the same coefficient and indicated good agreement between those two methods. We found that the profiles obtained by those two methods closely followed each other over most of the water depth, thus confirming the observations by Townsend (1976) of a constant ratio between Reynolds stress and TKE. This indicates that $C_1 \approx 0{\cdot}19$ is a suitable constant. The TKE W′ method was difficult to apply. Profiles were reasonably linear in the outer layer, but showed a slight maximum at around $0{\cdot}3z/h$ and a marked decrease in the inner layer. We cannot recommend the TKE W′ method from our experience because the profile is linear only over a short range, making the extrapolation too uncertain. Kim *et al.* (2000) who suggested this method only confirm that the coefficient $C_2 \approx 0.9$ in their study by comparing the results with those of the Reynolds stress method at one level above the bed.

For the wall similarity method, the results are comparable to those of the TKE method. The estimates obtained for five experiments fall close to the 1:1 line (Figure 8), and the remaining four are within 10% of the line. For experiment 5, a larger deviation is seen. Results from this experiment may therefore be less reliable. The constant, $F_k = 0{\cdot}3$ that was initially proposed for smooth wall flow and confirmed in transitional rough beds (Hurther and Lemmin, 2000), can also be considered a suitable constant for the application of this method in rough-bed flow. Thus, the characteristics of turbulence in the intermediate layer ($0{\cdot}25 \leq z/h \leq 0{\cdot}7$) are independent of the bed roughness (Hurther and Lemmin, 2000). Due to the one-third power relationship, this method is not sensitive to even larger errors in the determination of the energy flux. Since it is easy to apply this method in the intermediate layer ($0{\cdot}25 \leq z/h \leq 0{\cdot}7$) which is well above the roughness layer, it may be a promising tool for estimating shear velocity under rough-bed flow conditions and particularly in field studies.

For the spectral method applied to the vertical velocity component, robust spectra with a well-defined inertial subrange were found at all levels. Compared to the Reynolds stress method, five estimates obtained by this method are higher (Figure 8), and two are lower. The vertical increase in u_* with distance from the bed (Figure 7) indicates that the choice of the reference level for the determination of the shear velocity is important. Kim *et al.* (2000) found an increase of 22% between the values at 14 cm and 44 cm above the bed. This was their largest difference between the estimates at the two levels for all methods that they applied. They indicate that the level of 44 cm was close to the upper boundary of the logarithmic layer. In our study, the increase over the logarithmic layer height is higher and may reach up to 50%. The profiles of the TKE W′ method also strongly increase over this layer (Figure 4). We could not establish an objective criterion for the determination of a reference level. Comparing results obtained by this method at different levels above the bed with those obtained by the other methods (Table I), it appears that an estimate at $\approx 0.1\ z/h$ comes closest to those resulting from other methods (Figure 8). We also found a maximum in the TKE profiles at around $0{\cdot}1z/h$ (Figure 4). Therefore a reference level near $0{\cdot}1z/h$ may be suitable for this method. However, roughness layer effects may come into play. Assuming that a level at around $0{\cdot}1z/h$ is most representative for spectral method estimates, the flow may be non-isotropic under these bed roughness conditions, thus deviating from the assumptions made in the derivation of Equation 17. Too close to the bed, the ranges of energy production and dissipation may not be fully separated (Kim *et al.*, 2000). In our study, we found that the inertial subrange was well developed in the spectra at $0{\cdot}1z/h$, indicating a clear range separation. Townsend (1976) pointed out that in shear flows over a solid boundary layer, an equilibrium layer of wall turbulence exists near the solid wall. Under comparable flow conditions in the same channel investigated here, Hurther *et al.* (2007) showed that an equilibrium layer exists in the near-wall layer, where generation and dissipation are about six times higher than in the outer layer. Further open-channel or river flow investigations should be carried out before this method can be recommended as a reliable tool for estimating shear velocity in rough-bed open-channel flow.

In this study, $\approx$ 90% of all u_* estimates fall into a range of ±20%. A similar range of variability between estimates obtained by different methods was reported by Kim *et al.* (2000) over a soft bottom in tidal estuary flows. Nezu and Nakagawa (1993) mention a range of ±30% when comparing results from the logarithmic profile method and the Reynolds stress method with the force balance method (Equation 1). They indicate that this range increased with increasing roughness size, whereas we found a smaller range from our detailed profile measurements.

For each experiment, shear stress was calculated from the mean u_* values (Table I), and the results are plotted in Figure 9 against the corresponding mean streamwise velocities. A quadratic relationship with $\tau \approx 4.59\ u^2$ was fitted to the points. Pope *et al.* (2006) found $\tau \approx 2\ u^2$ for fine sediments over the same velocity range and suggested that steeper curves can be expected with increasing roughness. Venditti *et al.* (2005) reported a non-linear increase of the boundary shear stress with increasing mean velocity over a sand bed. This calculation was repeated for each of the different methods. The following regression coefficients were determined: the highest coefficient

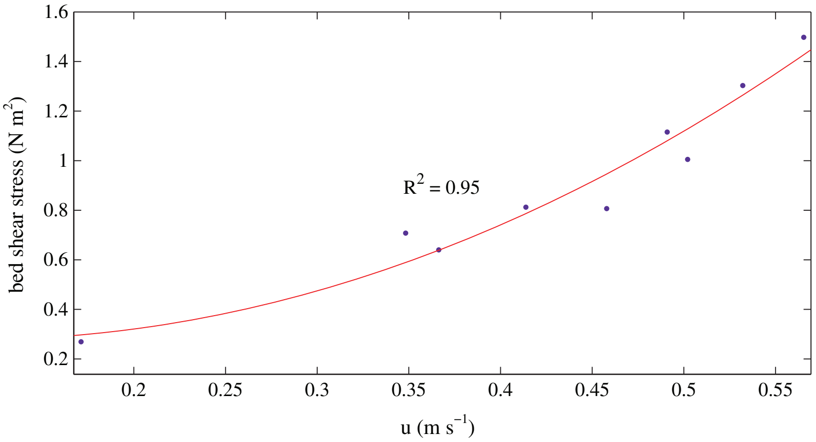

Figure 9. Relationship between shear stress averaged over all methods and mean streamwise velocity. This figure is available in colour online at wileyonlinelibrary.com/journal/espl

($R^2 = 0{\cdot}98$) was obtained for the wall similarity method, followed by $R^2 = 0{\cdot}90$ for the Reynolds stress method, $R^2 = 0{\cdot}83$ for the TKE method, and $R^2 = 0{\cdot}69$ for the log-law method.

We found reasonable agreement between the different shear velocity estimates for one fixed measurement location in the channel. In fully rough-bed flows, the spatial roughness distribution is irregular, and single location profiling may not provide shear stress estimates representative for a section, in particular for higher values of mean roughness and relative roughness. However, sediment dynamics is strongly influenced by local shear stress conditions and section mean values may not be representative (Wilcock, 1996). Monin and Yaglom (1971) pointed out that the form and mutual spacing of roughness elements may play a key role in local shear velocity dynamics.

Conclusion

In the present study, shear velocity was determined by five different methods in a flow over a fully rough bed of coarse gravel, where relative roughness is $D_{50}/h \approx 0{\cdot}075$. The analysis was based on ADVP measurements that provide quasi-instantaneous velocity profiles with high temporal and spatial resolution. The difficulties and advantages of the different methods were investigated. In rough-bed flows, problems may arise in precisely determining the location of the bed reference level or in the restricted range of validity of the different methods due to the underlying assumptions. It appears best to analyze velocity profile data by different methods. As indicated in this study, in addition to the shear velocity estimate, each method provides supplementary information about the flow characteristics, such as the thickness of the roughness layer, and the two-dimensionality of the mean flow. This information may in turn help to better define and understand the flow field conditions.

All methods provide comparable results for shear velocity. For comparable flow conditions, significant variability in the shear velocity estimates (Table I) by the logarithmic profile method was observed. Local and temporal variation in the loose bed roughness may contribute to the variability between experiments. The Reynolds stress method gave consistent results. For the TKE method, we found comparable results with the coefficient $C_1 = 0{\cdot}19$. Reynolds stress profiles and normalized TKE profiles closely follow each other over most of the water column with a constant ratio between the two profiles. The wall similarity concept was valid over a wide range of the water column ($0{\cdot}25 \leq z/h \leq 0{\cdot}7$) using the constant $F_k = 0{\cdot}3$. For the spectral method applied to the vertical velocity component, we were unable to objectively identify the level at which the method could be applied. Further studies are needed before this method can be recommended for use in rough-bed open-channel flow. Mean shear stress for all experiments follows a quadratic relationship with the mean velocity in the flow.

Since the TKE profiles were found to be fairly smooth, it may be of interest to explore the TKE method further for the determination of shear velocity in rough-bed flow studies and in rivers. The wall similarity method seems to be well suited for estimating shear velocity in these flows. It provides for a simplification with increased accuracy in the determination of shear velocity in difficult flow conditions. This method allows for the determination of u_* from a single point measurement at one level in the intermediate range ($0{\cdot}3 < h < 0{\cdot}6$).

Acknowledgments—This study was sponsored by European Commission contract no. 022441 (RII3) HYDRALAB-III. The authors are grateful for the support. The technical assistance of Claude Perrinjaquet is greatly appreciated. Constructive comments made by two anonymous reviewers helped to improve the manuscript.

Notation

D_p	= grain size for which the percentage p of a sample of bed material is finer (cm)
D_{50}	= grain size for which 50% of a sample of bed material is finer (cm)
h	= water depth (cm)
κ	= von Karman's constant
p	= turbulent energy production
u, v, w	= local mean longitudinal, transverse and vertical velocity (cm s^{-1})
u_*	= shear velocity (cm s^{-1})
u', v', w'	= local fluctuating longitudinal, transverse and vertical velocity (cm s^{-1})
overbar	= time mean values
$\bar{U}$	= 0.75 U_{max} (cm s^{-1})
U_{max}	= maximum velocity in the profile (cm s^{-1})
z_0	= characteristic hydraulic friction length (cm)
z	= vertical axis (cm)
f	= frequency (s^{-1})
ρ	= water density (kg m^{-3})
τ	= bed shear stress (kg s^{-2})
$\varphi_{ii}(k)$	= spectral density of the ith velocity component at wave number k

α_i = 1D Kolmogorov constant
ε = turbulent energy dissipation
σ_D = standard deviation of the bed roughness elements.

References

Albayrak I, Lemmin U. 2011. Secondary currents and corresponding surface velocity patterns in a turbulent open-channel flow over a rough bed. *Journal of Hydraulic Engineering ASCE* **137**: 1318–1334.

Biron PM, Robson C, Lapointe MF, Gaskin SJ. 2004. Comparing different bed shear stress estimates in simple and complex flow fields. *Earth Surface Processes and Landforms* **29**: 1403–1415.

Blanckaert K, Lemmin U. 2006. Means of noise reduction in acoustic turbulence measurements. *Journal of Hydraulic Research* **44**: 1–37.

Dombroski DE, Crimaldi JP. 2007. The accuracy of acoustic Doppler velocimetry measurements in turbulent boundary layer flows over a smooth bed. *Limnology and Oceanography: Methods* **5**: 23–33.

Ferreira RML, Franca MJ, Leal JGAB, Cardoso AH. 2012. Flow over rough mobile beds: friction factor and vertical distribution of the longitudinal mean velocity. *Water Resources Research* **48**: W05529. DOI. 10.1029/2011WR0111126

Franca M, Lemmin U. 2006. Eliminating velocity aliasing in acoustic Doppler velocity profiler data. *Measurement Science and Technology* **17**: 313–322.

Grant WD, Williams III AJ, Glenn SM. 1984. Bottom stress estimates and their prediction on the northern California continental shelf during CODE-1: the importance of wave–current interaction. *Journal of Physical Oceanography* **14**: 506–527.

Hinze JO. 1975. *Turbulence*. McGraw-Hill: New York.

Hurther D, Lemmin U. 2000. Shear stress statistics and wall similarity analysis in turbulent boundary layers using a high-resolution 3D ADVP. *Journal of Oceanic Engineering, IEEE* **25**: 446–457.

Hurther D, Lemmin U. 2001. A correction method of mean turbulence measurements with a 3D acoustic Doppler velocity profiler. *Journal of Atmospheric and Oceanic Technology* **18**: 446–458.

Hurther D, Lemmin U, Terray EA. 2007. Turbulent transport in the outer region of rough-wall open-channel flows: the contribution of large coherent shear stress structures (LC3S). *Journal of Fluid Mechanics* **574**: 465–493.

Kaimal JC, Wyngaard JC, Izumi Y, Cote OR. 1972. Spectral characteristics of surface-layer turbulence. *Quarterly Journal of the Royal Meteorological Society* **98**: 563–589.

Katul G, Wiberg P, Albertson J, Hornberger G. 2002. A mixed layer theory for flow resistance in shallow streams. *Water Resources Research* **38**: 1250. DOI. 10.1029/2001WR000817

Kim SC, Friedrichs CT, Maa JPY, Wright LD. 2000. Estimating bottom stress in a tidal boundary layer from acoustic Doppler velocimeter data. *Journal of Hydraulic Engineering ASCE* **126**: 399–406.

Lhermitte R, Lemmin U. 1994. Open channel flow and turbulence measurement by high resolution Doppler sonar. *Journal of Atmospheric and Oceanic Technology* **11**: 1295–1308.

Lopez F, Garcia MH. 1999. Wall similarity in turbulent open channel flow. *Journal of Engineering Mechanics* **125**: 789–796.

MacVicar BJ, Roy AG. 2007. Hydrodynamics of a forced riffle pool in a gravel bed river: 1. Mean velocity and turbulence intensity. *Water Resources Research* **43**: W12401. DOI. 10.1029/2006WR005272

Monin AS, Yaglom AM. 1971. *Statistical Fluid Mechanics*. Vol. **1**. MIT Press: Cambridge, MA.

Nezu I, Nakagawa H. 1993. *Turbulence in Open-channel Flows*. A.A. Balkema: Rotterdam.

Nicholas AP. 2001. Computational fluid dynamics modeling of boundary roughness in gravel bed rivers: an investigation of the effects of random variability of bed elevation. *Earth Surface Processes and Landforms* **26**: 345–362.

Nikora VI, Goring D. 2000. Flow turbulence over fixed and weakly mobile gravel beds. *Journal of Hydraulic Engineering ASCE* **126**: 679–690.

Nikora VI, Smart GM. 1997. Turbulence characteristics of New Zealand gravel-bed rivers. *Journal of Hydraulic Engineering ASCE* **123**: 764–773.

Pope ND, Widdows J, Brinsley MD. 2006. Estimation of bed shear stress using the turbulent kinetic energy approach – a comparison of annular flume and field data. *Continental Shelf Research* **26**: 959–970.

Raupach MR. 1981. Conditional statistics of Reynolds shear stress in rough-wall and smooth-wall turbulent boundary layers. *Journal of Fluid Mechanics* **108**: 363–382.

Raupach MR, Antonias RA, Rajagopalan S. 1991. Rough-wall turbulent boundary layers. *Applied Mechanics Reviews* **44**: 1–25.

Rowinski PM, Aberle J, Mazurczyk A. 2005. Shear velocity estimation in hydraulic research. *Acta Geophysica Polonica* **53**: 567–583.

Schlichting H. 1987. *Boundary-layer Theory*. McGraw-Hill: New York.

Shen C, Lemmin U. 1997. A two-dimensional acoustic sediment flux profiler. *Measurement Science and Technology* **8**: 880–884.

Smart GM. 1999. Turbulent velocity profiles and boundary shear in gravel bed rivers. *Journal of Hydraulic Engineering ASCE* **125**: 106–116.

Soulsby RL. 1980. Measurements of the Reynolds stress components close to a marine sand bank. *Marine Geology* **42**: 35–47.

Stapleton KR, Huntley DA. 1995. Seabed stress determination using the inertial dissipation method and the turbulent kinetic energy method. *Earth Surface Processes and Landforms* **20**: 807 – 815.

Tennekes H, Lumley JL. 1972. *A First Course in Turbulence*. MIT Press: Cambridge, MA.

Townsend AA. 1976. *The Structure of Turbulent Shear Flow*. Cambridge University Press: New York.

Venditti JG, Church MA, Benett SJ. 2005. Bed form initiation from a flat sand bed. *Journal of Geophysical Research* **110**: F01009. DOI. 10.1029/2004JF0000149

Wilcock PR. 1996. Estimating local bed shear stress from velocity observations. *Water Resources Research* **32**: 3361–3366.

Wilkinson RH. 1983. A method for evaluating statistical errors associated with logarithmic velocity profiles. *Geo-Marine Letters* **3**: 49–52.

Wolf J. 1999. The estimation of shear stresses from near-bed turbulent velocities for combined wave-current flows. *Coastal Engineering* **37**: 529–543.

Yaglom AM. 1979. Similarity laws for constant-pressure and pressure-gradient turbulent wall flows. *Annual Review of Fluid Mechanics* **11**: 505–540.